Acta Technica *62*, No. 3B/2017, 41–52

Vibration characteristic of aloft working vehicle under wind loading[1]

Jiang Hongqi[2], Li Shuncai[2]

Abstract. As the working height increases, the influences of the wind load on the vibration of aloft working vehicle become more significant. Nowadays, lesser research is conducted on the response of the aloft working vehicle to wind vibration, and the wind vibration response characteristic of this kind of structure is not clear yet. According to Davenport wind speed spectrum simulation, the pulse wind load is obtained, and it has been applied to the finite element model of the aloft working vehicle. Wind vibration characteristic analysis is conducted on the GKZ folding type aloft working vehicle at the maximum working height.The displacement and acceleration response of the aloft working vehicle under wind load is obtained, and further analysis reveals the frequency-domain characteristic. The results indicate this folding type working vehicle's wind induced response is mainly along wind; frequency-domain characteristic shows that this kind of working vehicle is sensitive to low-order frequency; field measurement of wind induced vibration agrees with the simulation results.

Key words. Aloft working vehicle, wind load modeling, time-domain characteristic, frequency-domain characteristic.

1. Introduction

Aloft working vehicle is a specialized vehicle used for transporting people and cargoes into a certain height to conduct aloft working. It has been widely used in industries of building, municipal constructions, fire control and etc. Most of research on this kind of vehicle focuses on the strength analysis and optimization of the working arm, stability analysis of the working vehicle as well as the leveling system. Literature [1], [2] utilized the finite element analysis method to conduct stress, deformation and model analysis of the telescopic arm of the aloft working vehicle. Also,the structure optimization was carried out and improvement method was proposed for weak load-bearing points. Literature [3], [4] developed a parametric software for

[1]This research is financially supported by the College Natural Science Foundation of Jiangsu Province National Natural Science Foundation of China under grant number 16KJB460010.

[2]School of Mechanical & Electrical Engineering, Jiangsu Normal University, Xuzhou, 221116, China; e-mails: jianghq@jsnu.edu.cn,zsclsc@263.net

straight arm aloft working vehicle design based on structure optimization design algorithm. Literature [5]–[7] conducted research and simulation on the leveling system of aloft working vehicle based on the technology of mechanical-electrical-hydraulic integration. Teng Ru Ming [8] employed the Lagrange's equation to establish the dynamic model of straight-arm aloft working vehicle and discussed the influences of boom parameters on the whole-body vibration of the working vehicle; Literature [9] utilized the method of structural mechanics to study the relationship between lifting speed,load and working platform vibration; Yin Shi Rong [10] obtained the movement law of the working platform as well as the driving moment varying pattern of each joint through dynamic motion simulation. Recently,the working height of various kinds of aloft working vehicle keeps increasing and the slenderness ratio of the working arm increases as well,which make them more sensitive to the wind load. The wind load also becomes one of the major loads that controls the vehicle design. Nowadays,lesser research is conducted on the wind vibration induced response of this type of machinery and there are still some urgent problems to be addressed in studying the characteristics of the response of this type of structure to wind load. This paper utilized the FEM software of ANSYS to conduct simulations of the dynamic characteristics of GKZ folding type aloft working vehicle under wind load and the displacement and acceleration responses of the aloft working vehicle are obtained. Furthermore, the frequency domain characteristics of this type of vehicle is obtained. Through field measurement of wind vibration response, the reliability of the simulation is verified and it can provide useful reference for the wind resistant design.

2. Wind load simulation

Aloft working vehicle is mainly based on boom structure, the premise of wind load simulation on the boom is to sample sufficient data of multi-dimension pulse wind. Nowadays, auto-regression (AR) model is commonly used to sample and process pulse wind data, due to algorithm's accuracy and calculation speed.

AR model can predict data by using existing continuous sampled data. Basic idea of AR model is, firstly, a set of random numbers with white spectrum are generated, the average of these numbers being 0. Then, this set of numbers is used as input of AR filter, the expected output is a set of random numbers with specific spectrum, which is the series of wind load history data. For example, wind speed or wind pressure history can be used to generate the specific spectrum. The detailed AR model algorithm is as follows [11].

A set of independent random process is generated; the expression is:

$$u(t) = \sum_{k=1}^{P} \Psi_k u(t - k\Delta t) + \sigma_{\mathrm{N}} N(t), \ k = 1, 2, \cdots, P. \tag{1}$$

Here, Δt is the time step, p is the auto-regression order, $N(t)$ is a set of normal-distribution number with average value 0 and variance value 1, σ_{N} is the root of the

variance, and Ψ_k is the auto-regression parameter, which is decided by

$$R_{\mathrm{u}}(j\Delta t) = \sum_{k=1}^{P} R_{\mathrm{u}}[(j-k)\Delta t]\Psi_k,\ j = 1, 2, \cdots, P, \tag{2}$$

where $R_{\mathrm{u}}(j\Delta t)$ is the auto-regression function

$$R_{\mathrm{u}}(j\Delta t) = \int_0^{\infty} S_{\mathrm{u}}(n)\cos(2\pi n j\Delta t)\,\mathrm{d}n, \tag{3}$$

where $S_{\mathrm{u}}(n)$ is the spectrum of pulse wind speed and σ_{N} can be generated by the following expression after Ψ_k is solved:

$$\sigma_{\mathrm{N}}^2 = R_{\mathrm{u}}(0) - \sum_{k=1}^{P} \Psi_k R_{\mathrm{u}}(k\Delta t)\ . \tag{4}$$

So far,we only include self spectral density of wind speed to calculate $u(t)$. However, because of thin and long boom on aloft working vehicle, we should also consider space relevance, that is, the cross spectral density.

Suppose pulse wind is a stationary Gaussian random process with zero mean, and the correlation matrix of multi-variable wind speed is

$$[R] = \begin{bmatrix} R_{11} & R_{12} & \cdots & R_{1n} \\ R_{21} & R_{21} & \cdots & R_{2n} \\ \vdots & \vdots & \ddots & \vdots \\ R_{n1} & R_{n2} & \cdots & R_{nn} \end{bmatrix}, \tag{5}$$

where $R_{ij} = \int_0^{\infty} S_{ij}(n)\,\mathrm{d}n$. Matrix $[R]$ can be Cholesky factorized as $[R] = [C][C]^{\mathrm{T}}$, $[C]$ being a lower triangular matrix, each element of which being resolved by the following expression

$$C_{ij} = \frac{R_{ij} - \sum_{k=1}^{j-1} C_{ik}C_{jk}}{C_{jj}},\ C_{ii} = \sqrt{R_{ii} - \sum_{k=1}^{i-1} C_{ik}^2}\,. \tag{6}$$

As a result, pulse wind speed vector is represented as

$$\{v_j(t)\} = [C]\{u_j(t)\}\ . \tag{7}$$

In our study, Davenport wind speed spectrum is chosen as characteristic spectrum, wind speed is set as 5 m/s at the height of 10 m. The ground roughness index is 0.16, sampling rate is 100 Hz, simulation time length is 300 s, time step is 0.1 s, and AR order is 4. At the head of boom and oil cylinder connecting points, 10 sample locations are set. The coordinate of sample location is decided by elevation of working arm.Wind speed vector of the 10 sample locations can be acquired by AR model

in the condition that aloft arm is working in the biggest operation altitude. Figure 1 shows the wind speed curve. Simulation spectrum of wind velocity time history power spectrum compared with the target power spectrum have good consistency, which is depicted in Fig. 2.

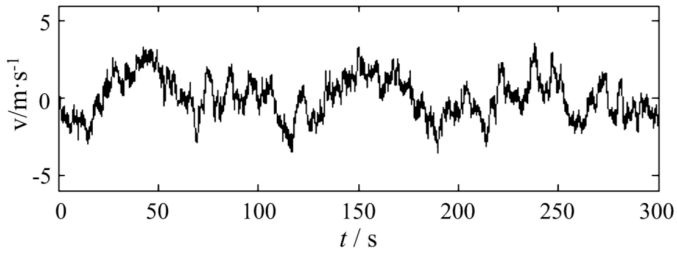

Fig. 1. Wind speed time travel curve

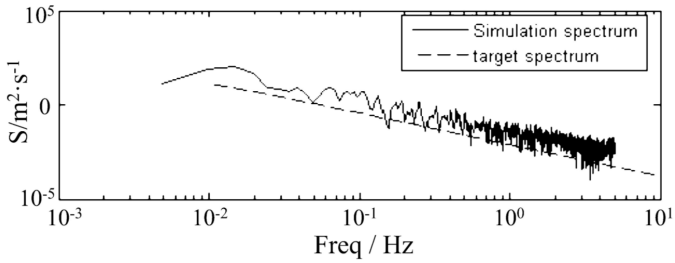

Fig. 2. Contrast of self-power-spectrum

According to simulation result of wind speed, the corresponding normal wind load is [12]

$$P = \frac{1}{2}\rho\mu_{\mathrm{s}}A_{\mathrm{i}}v_{\mathrm{i}}^2\,, \tag{8}$$

where, ρ is the air density, μ_{s} is the node average wind pressure coefficient, which is usually acquired by wind tunnel test and A_i is the node area.

3. Numerical simulation of wind-induced vibration response on aerial platform

3.1. Finite element model of aloft working vehicle

GLZ17 aloft working vehicle includes upper sub-arm and lower sub-arm,which are both soldered by 16 mm steel plate and hinged through horizontal pins. And upper sub-arm also contains a working platform. When working, two arms are stretched to a certain angle, sending crews and materials to the working platform.

The finite element model is built by ANSYS. The upper and lower sub-arms are modeled by shell163, arm connection and oil cylinder pin are modeled by beam 188, oil cylinder arm lifting is modeled by link 4, working platform is modeled by shell

unit. This model can simulate aloft working vehicle structure accurately. The finite element model is shown in Fig. 3.

Fig. 3. Finite element model of aloft working vehicle

Translation and rotation freedom degrees of reamings on lower sub-arm's tail and oil cylinder are restricted. Based on practical use of aloft working vehicle, the maximum working height is set. Calculated by Lonczos methodology, natural frequency and vibration mode are listed in Table 1.

Table 1. Frequency modal

Order	1	2	3	4	5	6	7	8
Frequency/Hz	1.08	4.06	6.95	10.78	18.80	26.21	39.29	45.33

3.2. Time domain characteristic of wind-induced vibration in aloft working vehicle

Loading program written by Ansys APDL language is used to apply simulated pulse wind load to finite element model of aloft working vehicle. Wind direction is vertical to working plane, and working vehicle is at maximum working height. According to analysis of wind-induced vibration response, displacement and acceleration curves in along-wind directions and vertical directions of working platform are shown in Figs. 4 and 5.

Figures 4 and 5 show that displacement and acceleration responses are both random processes with zero-mean, at the beginning of wind pulse load, acceleration response is more severe, then response tends to be stable but still random after 10 seconds due to damping. the response root mean squares of the displacements along wind direction on the operating platforms under two different working conditions are 1.71 mm and 14.9 mm/s^2, respectively. The response of vertical displacements and accelerations are smaller than that of wind directions.

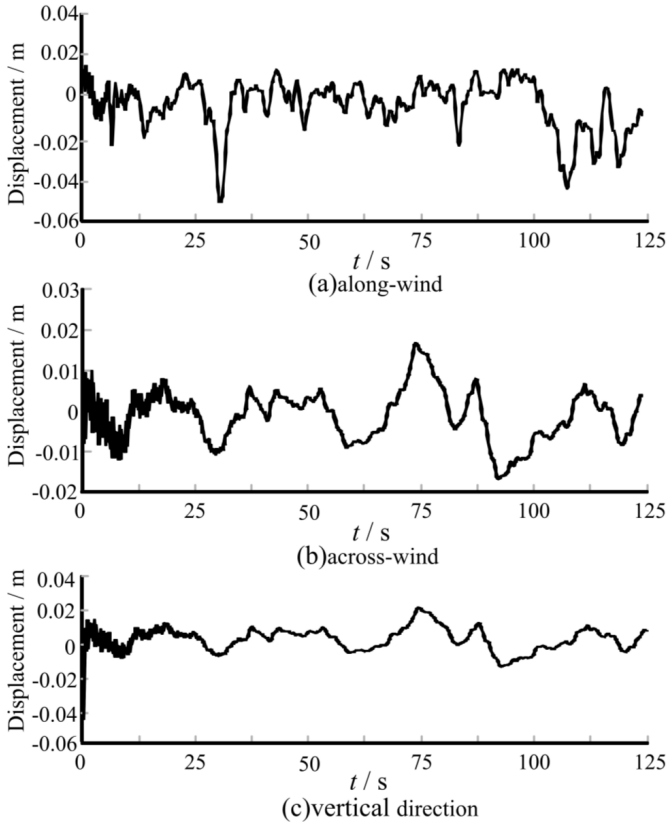

Fig. 4. Displacement-response time-history curves

3.3. Frequency domain characteristic of wind-induced vibration in aloft working vehicle

After Fourier transformation of time domain displacement and acceleration results under the two different working conditions, frequency domain results are shown in Figs. 6 and 7, respectively.

Figures 6 and 7 show that in the maximum working height, displacement and acceleration responses both have two resonance peak in frequency of 1.1 Hz and 6.9 Hz, corresponding to the first and third order mode. For displacement response,first order vibration mode gives the most contribution, and then the third order. The situation is reverse for acceleration response.

4. Measurement of the wind vibration induced response for the aloft working vehicle

To verify the accuracy of the numerical simulation and calculation, the GKZ17 aloft working vehicle is tested in a wind induced vibration filed measurement. Dur-

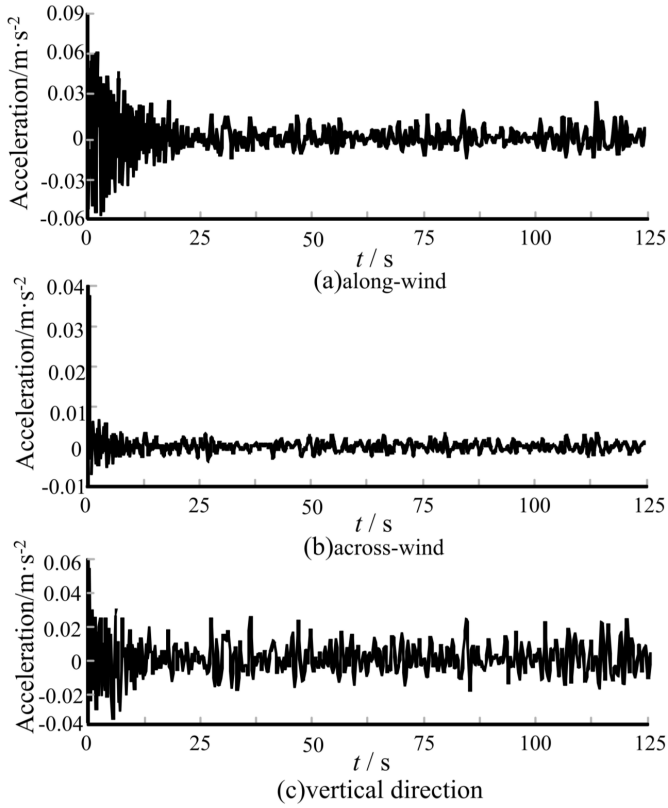

Fig. 5. Acceleration response time-history curves

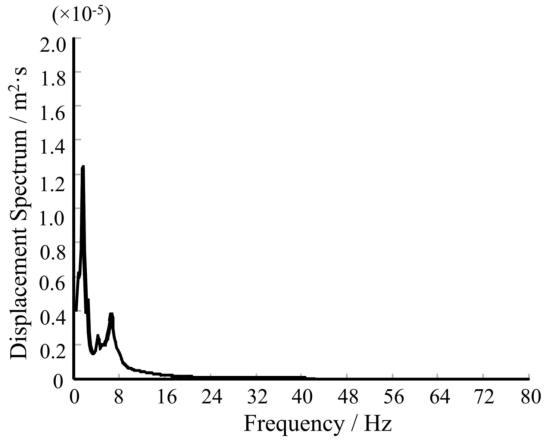

Fig. 6. Displacement response spectrum

ing the measurement, a north wind had the category 4 wind force and the weather condition is good. The wind is applied perpendicular to the work plane and the

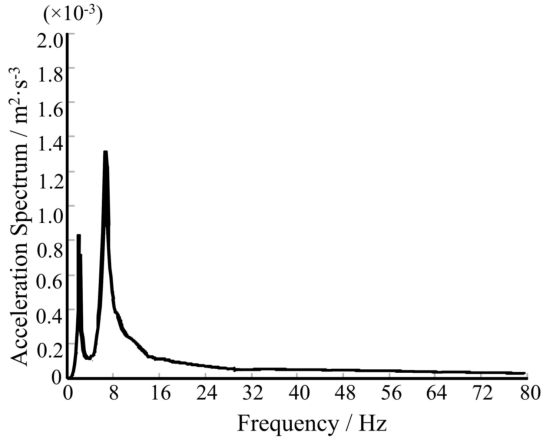

Fig. 7. Acceleration response spectrum

sampling time is 8 minutes for each test. Figures 8 and 9 are the measured displacement and acceleration curves. Figure 10 and 11 are the measured displacement and acceleration power spectra. From these figures, the base frequency at the maximum working height is 0.854 Hz which is slightly lower than model analysis result and caused by the model and measurement errors. However, according to displacement and acceleration power spectrum analysis, peak response characteristics mostly agree with the simulation results which means the theoretical analysis model and its results are reliable.

Table 2 lists the measured root mean squares of the displacement and acceleration responses in the along wind, vertical and cross wind directions. These results are compared with the simulation results.

Table 2. Simulation value compared with the measured values

	Mean square root of displacement (mm)		Mean square root of Acceleration (mm/s^2)	
	Simulation value	Measured value	Simulation value	Measured value
Along-wind direction	1.71	1.19	14.9	13.1
Across-wind direction	0.15	0.42	2.06	11.21
Vertical direction	0.65	0.12	4.63	6.77

From Table 2, the major response of this type of aloft working vehicle to wind vibration at the maximum working height is along wind and the displacement and acceleration at the vertical and cross wind directions are minor. Measured along wind displacement and acceleration are close to the simulation results; however, the differences between measurements and simulations in the vertical and cross wind directions are relatively large. This is caused by the model error and measurement

error and also the uncertainty of the measured wind direction and speed makes another important factor.

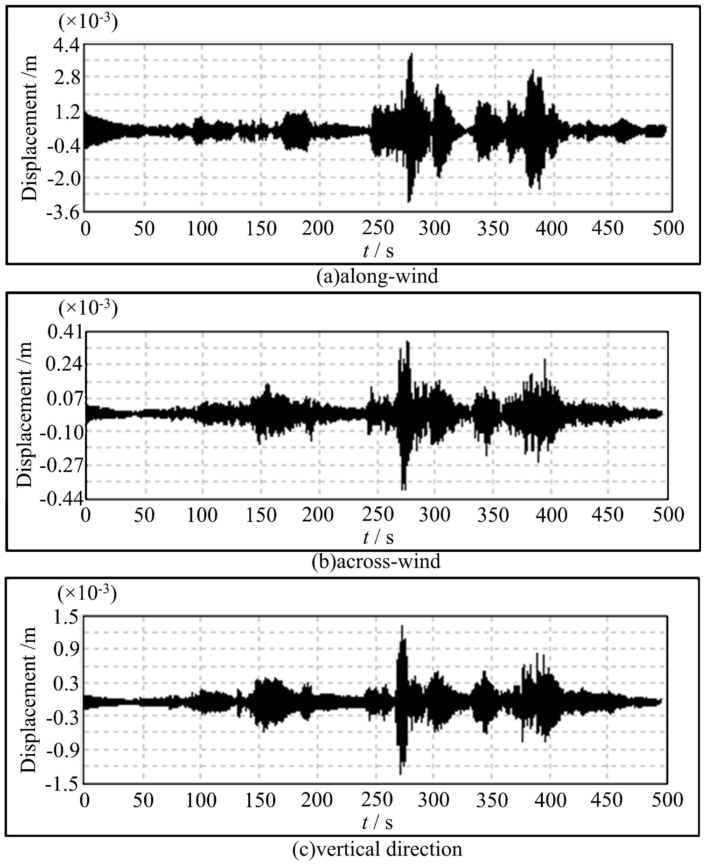

Fig. 8. The in-site test time-history curves of displacements

5. Conclusion

This paper utilizes the Davenport wind speed spectrum that does not change with height to simulate the wind load applied on the aloft working vehicle. A certain type of folding type aloft working vehicle is chosen as analysis example. A wind load is applied perpendicular to the working plane with a speed of 5 m/s and the time domain and frequency domain analysis of the wind vibration induced response at the maximum working height are conducted. The vibrating response of the aloft working vehicle work platform under wind load stimulation is obtained and furthermore is verified via field measurement. Major conclusions are as follows:

(1) The wind vibration induced response of this type of aloft working vehicle is mainly along the wind, while the vertical and across-wind response are minor.

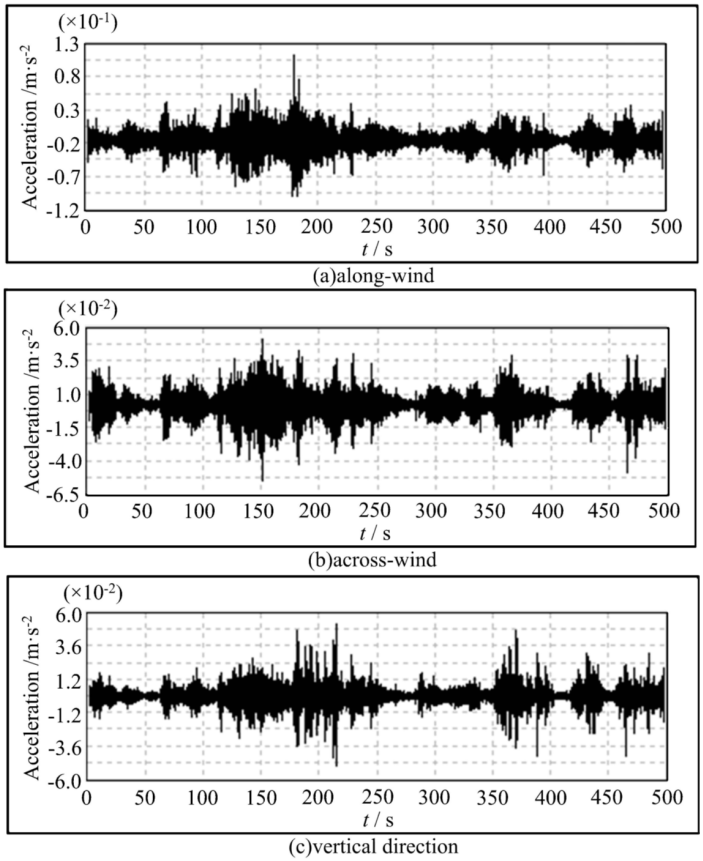

Fig. 9. The in-site test time-history curves of accelerations

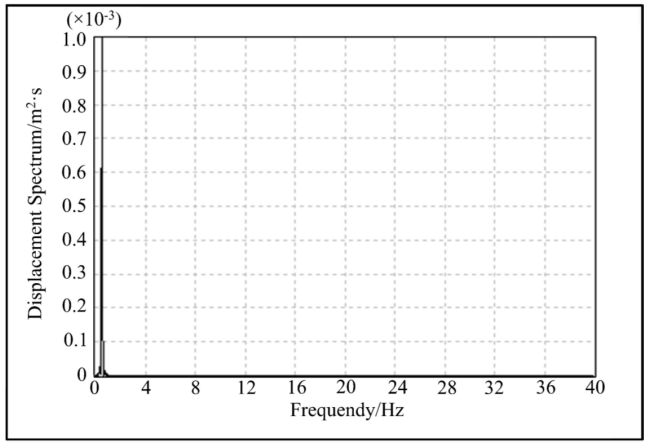

Fig. 10. The in-site test displacement spectrum

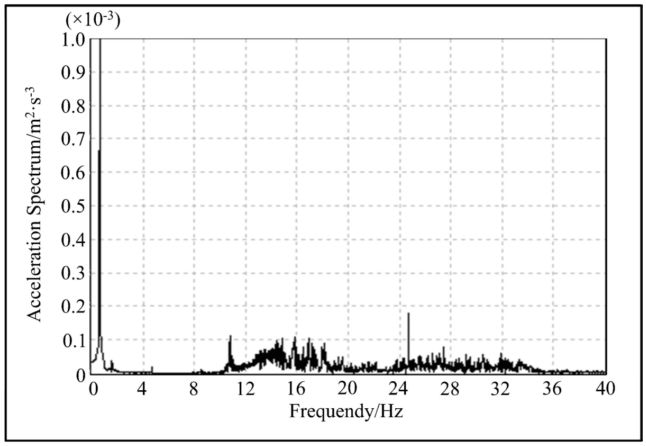

Fig. 11. The in-site test acceleration spectrum

(2) At the maximum working height, the root mean squares of the along wind displacement and acceleration response are 1.71 mm and 14.9 mm/s^2, respectively. The simulation results are slightly larger than the measured results.

(3) Through data processing of the time domain analysis, the frequency domain characteristic of this type of aloft working vehicle is obtained. The measured base frequency is slightly lower than the simulation result. But the peak response characteristic agrees with the simulation results, indicating that theoretical analysis model and its results are reliable.

References

[1] H. Q. Jiang, F. S. Wang: *Vibration mode analysis of crane jib using finite element method.* Transaction of the Chinese Society for Agricultural Machinery *37* (2006), No. 3, 20–22.

[2] T. R. Smith: *An evaluation of fatigue cracking in an aerial platform yoke from a fire-fighting vehicle.* Engineering Failure Analysis *9* (2002), No. 3, 303–312.

[3] D. W. Dong: *Auto-leveling mechanism of Simon–Cella working platform.* Road Machinery & Construction Mechanization *21* (2004), No. 6, 33–34.

[4] C. Su, L. N. Zhang, H. D. Xu: *The automatic leveling system of working platform on model CDZ50 elevating platform fire engine.* Construction Machinery and Equipment *35* (2004), No. 9, 23–25.

[5] F. L. Wang, J. Q. Xiong, Y. C. Liu: *Analysis of stability for folding type aerial platform.* Construction Machinery and Equipment (2011), No. 3, 23–28.

[6] W. C. Guo, C. Zhang, N. Xiao: *Research on the poured over performance of mast type aloft working car based on ADAMS.* Machinery Design & Manufacture (2011), No. 10, 266–268.

[7] Z. J. Dong, X. Wu, T. Luo, G. Xiong: *Telescopic boom transient dynamics analysis based on Rayleigh–Ritz method.* Machinery Design & Manufactiure (2015), No. 1, 184 to 186.

[8] R. M. Teng, X. Y. Cao, S. D. Gao, X. Wang: *Hybrid integrated design and realizable strategy of database of mechanical product gene.* International Conference on

Natural Computation, 10–12 August 2010, Yantai, Shandong, China, Published ICNC (2010), 4039–4044.

[9] T. H. Luo, W. W. Chen: *Research on stability of folding-telescopic arm for aerial work platform*. Machinery Design & Manufacture (2009), No. 9, 118–119.

[10] S. R. Yin, Y. Q. Jia, X. X. Yin: *On dynamics of aerial work platform lifting booms based on ADAMS*. Journal of Chongqing Jiaotong University (Natural Science) *30* (2011), No. 5, 1031–1034.

[11] L. Qin, J. J. Yuan, X. Y. Li: *Wind speed time-history simulation for transmission line system based on AR method*. Water Resources and Power *29* (2011), No. 2, 169 to 171.

[12] Y. Liu, X. Xu, X. J. Zhou: *Analysis of dynamic response and wind-induced vibration control of high-rising structure under typhoon*. Noise and Vibration Control *29* (2009), No. 2, 30–34.

Received April 30, 2017